Current Therapeutic Research 99 (2023) 100714

Contents lists available at ScienceDirect

Current Therapeutic Research

journal homepage: www.elsevier.com/locate/curtheres

Optimization of Nasal Liposome Formulation of Venlafaxine Hydrochloride using a Box-Behnken Experimental Design

Sulekha Khute, MPharm, Rajendra K. Jangde, PhD, MPharm*

University Institute of Pharmacy, Pt Ravishankar Shukla University, Chhattisgarh, India

ARTICLE INFO

Article history:
Received 8 April 2023
Accepted 10 August 2023

Key words:
Antidepressant
Intranasal
Liposome
Optimization
Venlafaxine

ABSTRACT

Background: Intranasal administration is among the most effective alternatives to deliver drugs directly to the brain and prevent first-pass metabolism. Venlafaxine-loaded liposomes are biocompatible carriers that enhance transport qualities over the nasal mucosa.
Objective: This research aimed to develop, formulate, characterize, and observe the prepared formulation.
Methods: The formulation was developed using the thin-film hydration technique. The response surface plot interrelationship between three independent variables are lipid, cholesterol and polymer and four dependent variables such as particle size, percentage entrapment efficiency, and percentage drug release were ascertained using the Box-Behnken design.
Results: The drug-release chitosan-coated liposomes were reported to have a particle size distribution, entanglement efficiency, and 84%, respectively, of 191 ± 34.71 nm, 94 ± 2.71% and 94 ± 2.71%. According to *in vitro* investigations, liposomes as a delivery system for the nasal route provided a more sustained drug release than the oral dosing form.
Conclusions: The intranasal administration of venlafaxine liposomal vesicles effectively enhanced the absolute bioavailability, retention time, and brain delivery of venlafaxine.

Introduction

Depression is a common and debilitating illness. Globally, it is the leading cause of disability, with significant negative influence on quality of life, mortality, morbidity, cognitive function, and general occurrence due to serotonin and norepinephrine deficiency.[1] According to the World Health Organization, depression will, during the next few years, overtake diabetes as the second-leading cause of the global health burden. Depression usually treated with classes of medications, particularly the tricyclic antidepressants and selective serotonin reuptake inhibitors. Depression is a devastating neurological disorder that affects millions of people worldwide.[1,2] Depression symptoms are frequently seen in people between the ages of 15 and 44 years, in both sexes.[3] Although depression is not a life-threatening condition, in the worst-case scenario, suicides have been reported.[4] The blood-brain barrier is a selectively semipermeable barrier between blood vessels and nerve tissue that maintains tissue function, regulates transport, and provides protection. It prevents bloodborne infections, leukocytes, and toxins from entering the brain while allowing selective passive transport of molecules like glucose, amino acids, and water to maintain brain homeostasis.[5] Venlafaxine (VLF) is a phenylethylamine derivative structurally related to the biogenic amines by blocking norepinephrine and dopamine in the brain cells for treating depression and anxiety disorders.[6] It is a white, crystalline substance that possesses venlafaxine water solubility qualities. Because of its limited bioavailability, it does not penetrate the biological membrane when taken orally and does not thereby alleviate depression. An oral dose of VLF can be given at doses ranging from 75 to 450 mg/d. It has demonstrated efficacy as a neuropathic pain reliever and has been shown to lessen premenstrual dysphoric disorder. It has provided a dual-action, more-effective treatment for resistant depression. VLF is effective in resistant depression and is better than selective serotonin reuptake inhibitors in preventing depression relapse.[7]

The nasal route is a quick and painless way to deliver medication to the brain through the nasal mucosa, aimed at treating central nervous system (CNS) disorders with minimal exposure to systemic blood flow.[8] The nasal system also includes blood vessels, cerebrospinal fluid, and lymphatic systems, which play an important role in a molecule's mobility from the nasal cavity and

* Address correspondence to: Rajendra K. Jangde, PhD, MPharm, University Institute of Pharmacy, Pt Ravishankar Shukla University, Raipur 492010, Chhattisgarh, India.
E-mail address: rjangdepy@gmail.com (R.K. Jangde).

https://doi.org/10.1016/j.curtheres.2023.100714

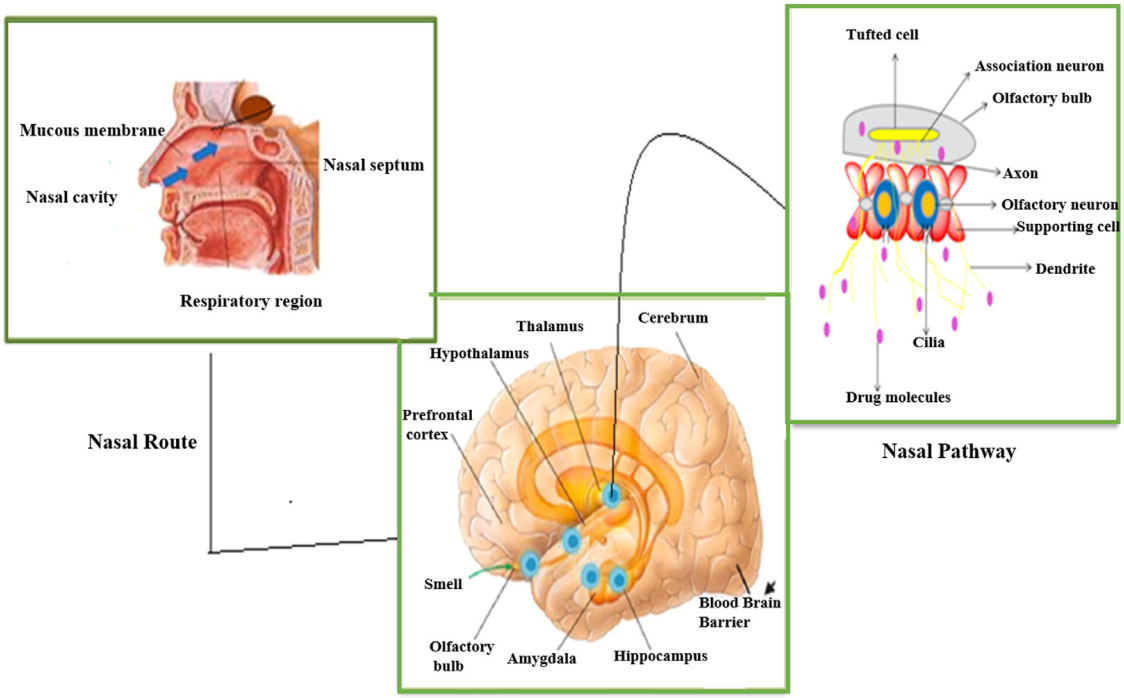

Figure 1. Intranasal drug delivery through the olfactory pathway to the central nervous system.

represent a potential delivery route to the brain.[9] These are the most significant alternative routes for delivering therapeutics to the brain due to numerous advantages such as rapid, targeted drug delivery and rapid onset of action in the CNS through the trigeminal and olfactory epithelium nerve pathways to reduce systemic side effects.[10] The olfactory receptor neurons contain cilia and are rapidly transported through the olfactory mucosa to the CNS via transcellular or paracellular pathways extending downward from the olfactory epithelium and transfer to the olfactory bulb. The mucus layer thickens during colds, decreasing olfactory sensibility.[11]

The olfactory glands produce lipids through mucous secretions to lubricate the olfactory epithelium and break down odorant-containing gases. The epithelium of this area consists of 3 distinct layers, including epithelial (supporting) cells, basal cells, and sensory neurons. This is the most popular and significant route of medication transport to the brain. Due to the specific fraction dose delivered to the CNS, most drugs are lost through enzymatic degradation or mucociliary clearance. The drugs encapsulated in liposomes (LPs) can easily enter the systemic circulation before excretion is distributed to nontarget tissues.[12] The nasal cavity is home to nasal tubercles, which are projections from the sidewalls of the nasal cavity that create turbinates. The nasal cavity consists of 4 different types of cells: basal cells, nonfibrous columnar cells, and fibrous columnar cells. Drug molecules reach the systemic circulation via the trigeminal canal of the nasal passage. This trigeminal nerve is most important for transmitting sensory information. Nasal administration provides rapid symptom relief related to CNS disorders with a more favorable side effect profile than oral, parenteral, or transdermal administration. A nasal drug delivery system is more effective when administered at relatively lower doses than locally, thereby reducing potential toxicity.[13,14] Intranasal drug delivery through the olfactory pathway to the CNS is illustrated in Figure 1.

LP drug delivery systems have attracted more attention owing to their numerous edges, like the encapsulation efficiency of lipophilic and hydrophilic molecules with a wide range of hydrophobicity levels. The pKa values target therapeutic agent release by modifying the liposomal surface, extending the therapeutic agent release, lowering clinical medication doses, and reducing adverse consequences.[15] LPs can be created in various shapes and layers (single, bilayer, or multiple layers), depending on the preparation techniques selected. Multilamellar vesicle formations emerge naturally when lipids are mixed with an aqueous solution. Sonication is typically used (using a probe-type or bath-type device) for unilamellar vesicles to reduce the size of Multilamellar vesicles and prepare tiny unilamellar vesicles. The intranasal method is among the most appealing ways to get medicines into your systemic circulation.[16] LPs are used as biocompatible carriers to enhance transport capabilities over the nasal mucosa. Stability is among the major issues that physically and chemically limit the widespread use of LPs. Depending on the composition, the final LPs formulation may be chemically and physically unstable, resulting in a short shelf life. Lyophilization, which involves lyophilizing the final LPs product with a cryoprotectant (often a sugar-like trehalose) and then reconstituting it with the vehicle immediately before administration, can solve these issues. The nasal cavity is lined with a layer of mucus and hair and is involved in the entrapment of inhaled formulations.[17]

There are different types of LPs, including conventional LPs, niosomes, ethosomes, and transfersomes in drug delivery.[18–21] Dose dumping, which raises the risk of toxicity, is the main disadvantage of sustained-release formulations.[22] Nasal drug delivery systems based on liposomal formulations have demonstrated unique qualities that enable them to overcome biological barriers and lead to enhanced pharmacodynamics. The obvious advantages of LPs include drug-loading a variety of molecules, reducing systemic and off-target toxicity, increasing the residence time of the drug in the bloodstream, dispersing the drug across the blood-brain barrier, and aiding in drug entry into the brain to achieve a desired outcome.[23–25] An important goal of LPs formulations is to alter the distribution and reduce the toxicity of drugs, allowing higher doses to be administered. In such cases, the development of bioanalytical methods to measure drug encapsulation and release is a con-

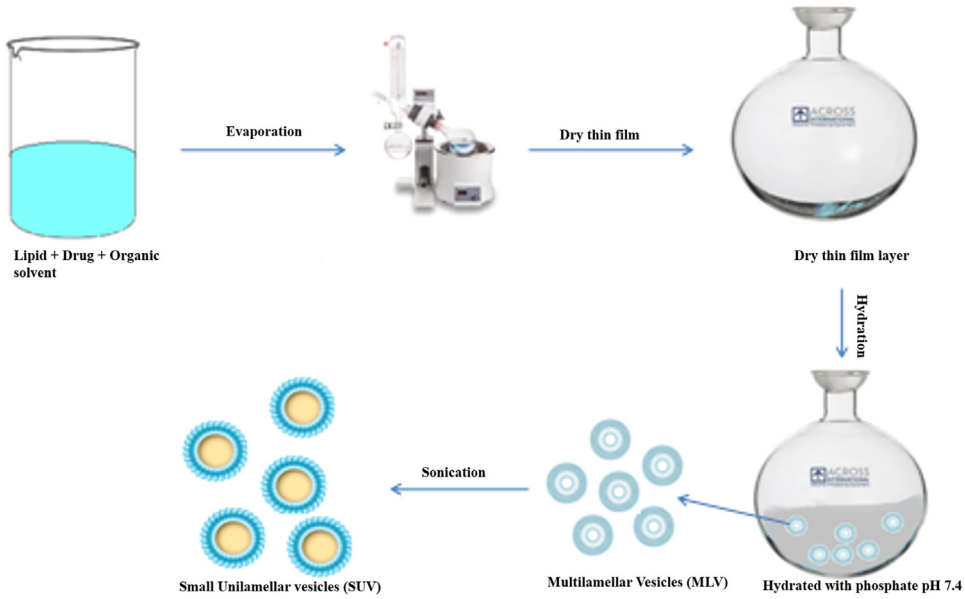

Figure 2. Preparation procedure for liposomes.

cern because of the potential for dose dumping, in the initial stage of the drug development may not be warranted.[26,27] VLF extended release is a first-line treatment for depression in older people due to fewer side effects, a lower potential for drug interactions, and better tolerability than other antidepressant classes.[28] The primary focus of this research was to prepare LPs of VLF hydrochloride by the thin film hydration (TFH) method and evaluate the effects of different excipients and the phosphatidylcholine to surfactant ratio on vesicle morphology, entrapment efficiency (EE), and *in vitro* drug release.

Materials and Methods

VLF hydrochloride was a gift sample from Zydus Cadila (Ahmadabad, India). Phosphatidylcholine, chitosan, and 1 kDa molecular weight cutoff dialysis membranes (Spectra, Por7) were purchased from HiMedia Laboratories, Mumbai, Maharashtra, India. Cholesterol was purchased from Loba Chemie Pvt Ltd, Mumbai, India. All other commercially available chemicals were of analytical grade.

Instrumentation

Zeta potential Zetasizer Nano ZS (Malvern Instruments, Worcestershire, United Kingdom) and UV-visible spectrophotometer (Shimadzu UV-1800, Kyoto, Japan). The Fourier-transform infrared (FT-IR) spectroscopy investigation was conducted using a spectrum analyzer from the National Centre for Natural Resources, Pt Ravishankar Shukla University. Differential scanning calorimeter (DSC) (DSC2500, PerkinElmer Instruments, USA), Scanning electron microscopy (FEI Quanta 200 ESEM FEG, Hillsboro, Oregon, USA), and Transmission electron microscopy (STEM; JEOL Ltd., Tokyo, Japan).

Formulation of LPs

The thin film technique was used to prepare VLF-loaded LPs. Briefly, the hydrophobic excipients, such as soy lecithin (60 mg) and cholesterol (2 mg), were dissolved in 5 mL chloroform. Then, the VLF (30 mg) and 10 mL of 1% chitosan solution were mixed in the above mixture solution and transferred into a suitable round-bottom flask as shown in Table 1. The flask was then attached to rotary evaporator (IKA RV 10, Werke, Staufen, Germany) and and a temperature of 37 to 41°C was maintained. A vacuum was applied to the rotating flask at about 160 rpm at 30°C to evaporate the chloroform, forming a uniform lipid film. The dried lipid film was kept under a vacuum overnight to remove excess chloroform. The lipid film was hydrated with 10 mL phosphate-buffered saline (pH 7.4) containing VLF until the lipid film was formed. The preparation procedure for the VLF-loaded LPs is illustrated in Figure 2.[18,19]

Table 1
Prepared formulations of liposomes were taken, providing a quantityof drug lipid concentration.

Serial No.	Excipient	Total amount (mg)
1	Drug concentration	30
2	Lipid concentration	60
3	Polymer concentration	1%

Table 2
The degree of independent and dependent factors that were chosen for Box-Behnken design to prepare venlafaxine hydrochloride-loaded liposomes.

A definitive coding value is used			
Factor	Low (−1)	Medium (0)	High (+1)
Independent			
X_1	6	12	18
X_2	0.5	2	3
X_3	0.5	1	2
Dependent			
Y_1	191	197	315
Y_2	64	90	94
Y_3	42	80	84

X_1 = Total lipid concentration; X_2 = cholesterol; X_3 = polymer; Y_1 = size (in nanometers); Y_2 = % entrapment efficiency; Y_3 = % drug release.

Optimization of LPs by Box-Behnken design

The required characteristics of the nano lipid carrier system for nasal distribution may be directly influenced by the total concentration of lipids, cholesterol, and polymers. All factors influencing formulation properties are included based on the results.[20] Three factors and a 3^2 Box-Behnken design (BBD) were used to optimize VLF. The observed responses for the BBD for optimizing VLF-loaded

Table 3
Box-Behnken design design for venlafaxine-loaded liposome formulation optimization based on observed responses.

Std	Run	Independent variables			Dependent variables		
		X_1	X_2	X_3	Y_1	Y_2	Y_3
13	1	0	0	0	260	83	66
14	2	0	0	0	191	89	70
10	3	0	+1	−1	315	64	81
15	4	0	0	0	195	92	75
1	5	−1	−1	0	200	69	42
6	6	+1	0	−1	193	93	83
5	7	−1	0	−1	210	70	69
16	8	0	0	0	196	90	72
12	9	0	+1	+1	292	75	83
17	10	0	0	0	197	91	74
11	11	0	−1	+1	201	64	80
7	12	−1	0	+1	192	93	72
2	13	+1	−1	0	212	79	82
3	14	−1	+1	0	315	69	79
8	15	+1	0	+1	191	94	84
4	16	+1	+1	0	288	64	43
9	17	0	−1	−1	192	78	63

Std = Standard; X_1 = total lipid concentration; X_2 = cholesterol; X_3 = polymer concentration; Y_1 = particle size (in nanometers); Y_2 = % entrapment efficiency; Y3 = % drug release).

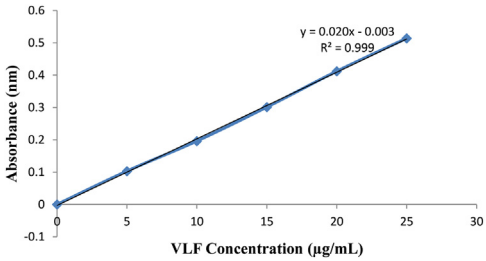

Figure 3. Standard calibration curve of venlafaxine.

LPs formulation factors that are independent and dependent variables are shown in Table 2. The design was deliberate, consisting of 17 investigational runs (as shown in Table 3).

The quadratic equation is as follows:

$$Y = b_0 + b_1X_1 + b_2X_2 + b_3X_3 + b_{12}X_1X_2 + b_{13}X_1X_3 + b_{23}X_2X_3 + b_{11}X_1^2 + b_{22}X_2^2 + b_{33}X_3^2$$

where Y is the observed dependent value for every factor level; b_0 is constant; b_1, b_2, and b_3 are linear coefficients, whereas b_{12}, b_{13}, and b_{23} are the interaction coefficients between the three factors. Thus, b_{11}, b_{22}, and b_{33} are the quadratic coefficients of the predicted values, and X_1, X_2, and X_3 are valued for the independent variables.[21]

Characterization of the prepared formulation

Standard calibration curve

The absorbance of the prepared sample was determined at 224 nm for the estimation of VLF. A volume of 100 µg/mL VLF absorbance was noted at 224 nm. The concentrations of the drugs were calculated by the equation of the standard curve method and double-point standardization. The following equation as; Y= Mx + C in which y is absorbance, m is slope, x is concentration, and c is the constant.

FT-IR

The compatibility formulated of VLF hydrochloride with phosphatidylcholine and cholesterol was determined using FT-IR.[28]

Particle size and the surface charge of particles

The mean particle size (PS) and zeta potential at 25°C were determined by dynamic light scattering with the Zetasizer Nano ZS. The formulations were adequately diluted with distilled water to produce an appropriate scattering intensity before the analysis.[29]

%EE

The VLF-loaded sample was taken at about 2 mL, then centrifuged at 15,000 rpm at 4 °C for 1 hour. The supernatant was collected and diluted up to 10 mL. The diluted supernatant was examined using the UV technique. The %EE was calculated using the following formula.[30]

$$EE\,\% = \left(\mathrm{Wi} - \mathrm{Ws}\right)/\left(\mathrm{Wi}\right) \times 100$$

where Wi refers to the weight of initial drug and Ws = weight of the supernatant.

Morphology study

SEM

SEM was implemented to analyze the morphology of the VLF-loaded LPs.[30] A drop of the LPs solution was applied to the gold-coated metal stubs under vacuum pressure and subjected to SEM analysis.

TEM

TEM was used to determine the morphology of the chosen VLF-loaded LPs.[31] A small amount of LPs was applied to the carbon-coated paraffin sheet and allowed to sit for 1 minute after being diluted in an appropriate solvent. The grid was prepared and dried at 37 °C and set with a drop of (0.2 % w/v) phosphotungstate for 10 seconds after TEM analyzed the sample.

Differential scanning calorimetry

A valuable quantity of dehydrated VLF samples was loaded and sealed into a differential scanning calorimetry pan. The sample was scanned between 40 and 400 °C at a heating rate of 5 °C/min under an inert nitrogen environment using differential scanning calorimetry.[32]

In vitro release studies

In vitro, drug release studies were performed using a dialysis membrane. A definite volume of the prepared LPs dispersion was filled into a dialysis bag up to 250 mL dissolution medium containing phosphate-buffered saline (pH 6.5) (molecular weight of dialysis bag cutoff: 12,000–14,000 DA), stirred with a magnetic stirrer

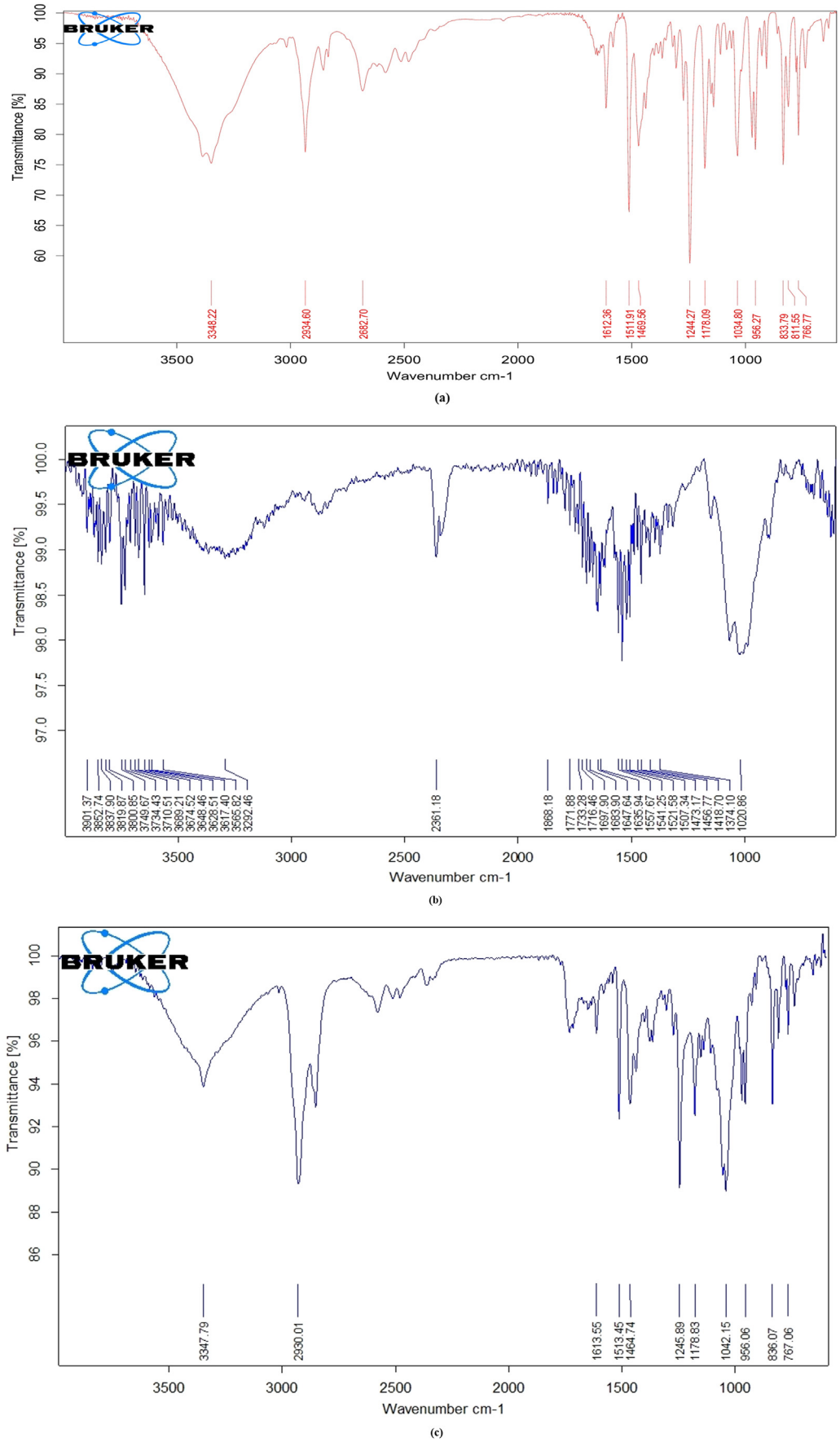

Figure 4. FT-IR spectra: Pure drug of venlaxafine (a), chitosan (b), and physical mixtures containing active pharmaceutical ingredients and excipients (c).

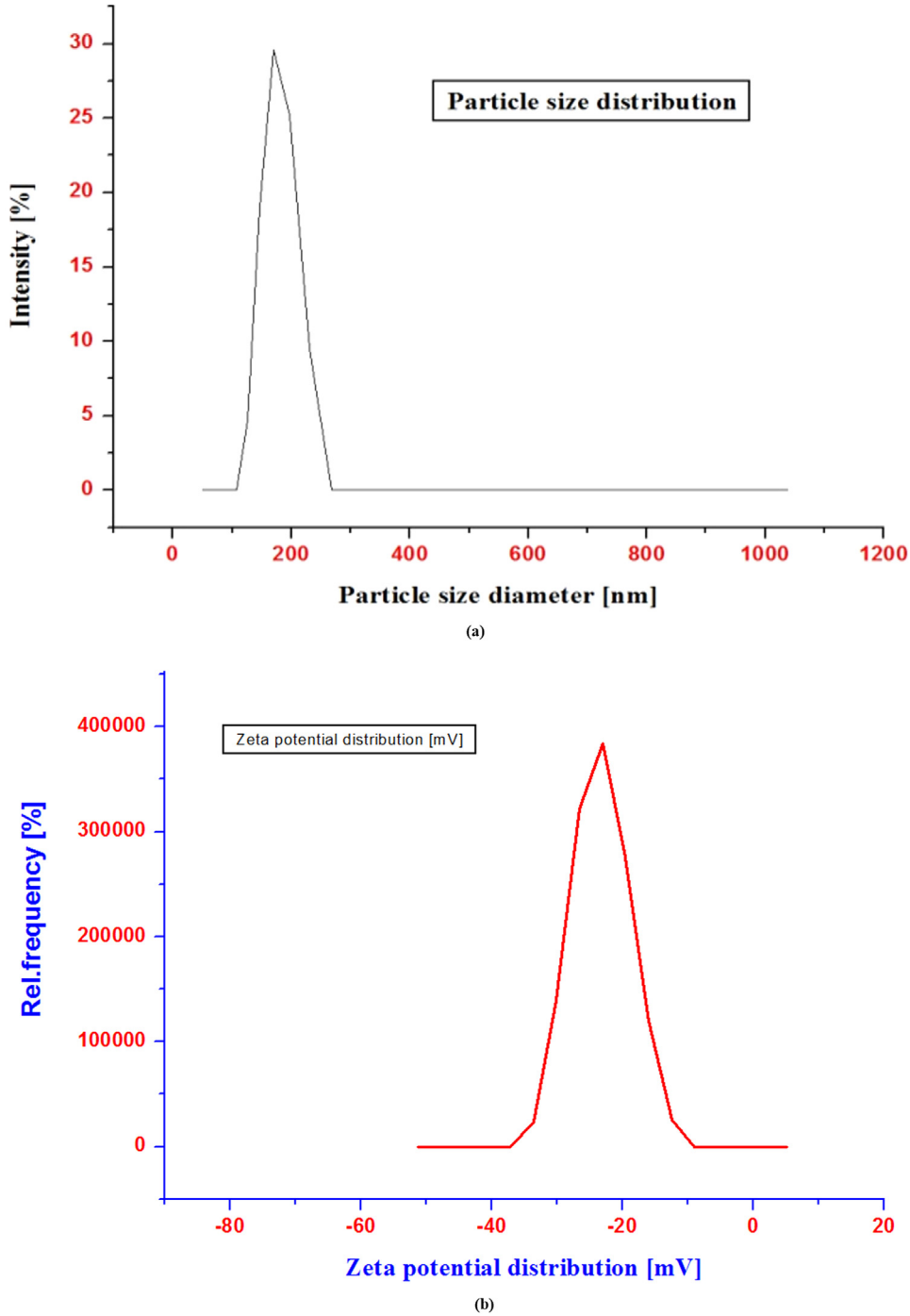

Figure 5. Particle size distribution graph (a) and zeta potential distribution graph (b).

at 100 rpm and maintained a temperature at 37 ° C. Aliquots of 2 mL were taken from phosphate-buffered saline at 30 minutes, 1, 2, 4, 6, 8, 10, 12, and 24 hours, and replaced with fresh 2 mL dissolution medium. Then the sample was analyzed spectrophotometrically at 224 nm (λmax for VLF). All samples were analyzed in triplicate, and the results were expressed as mean (SD).[33]

Results and Discussion

Standard calibration curve

VLF in phosphate buffered saline at pH 6.5 was measured absorbance range of 200 to 400 nm. Pure venlafaxine concentration was determined initially and further, all the excipients (chitosan, LPs, phosphatidylcholine, cholesterol, chitosan, and chloroform) were mixed with the VLF solution was determined using UV spectroscopy. The standard calibration curve of VLF was shown in Figure 3. There is no interaction between the excipients and pure VLF.

FT-IR spectroscopy

An FT-IR investigation was used to better understand the drugs and their excipient interactions. The FTIR spectra of VLF hydrochloride and a mixture of the drug with the final formulation showed a characteristic stretching band of N-H at 3349 cm^{-1}, aliphatic C-H

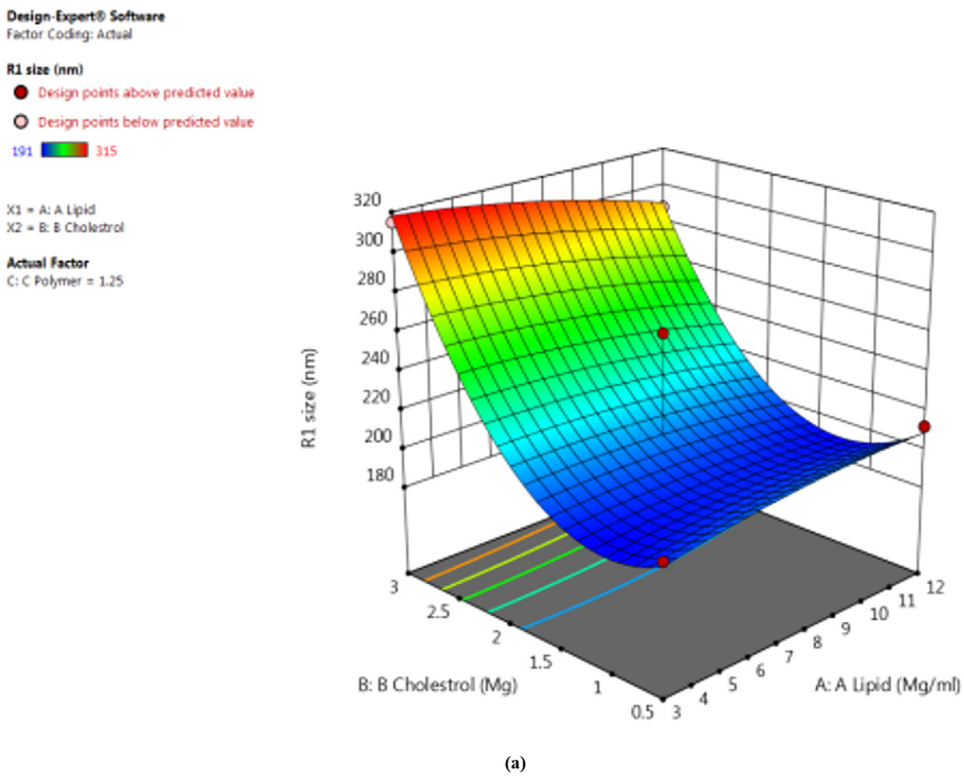

(a)

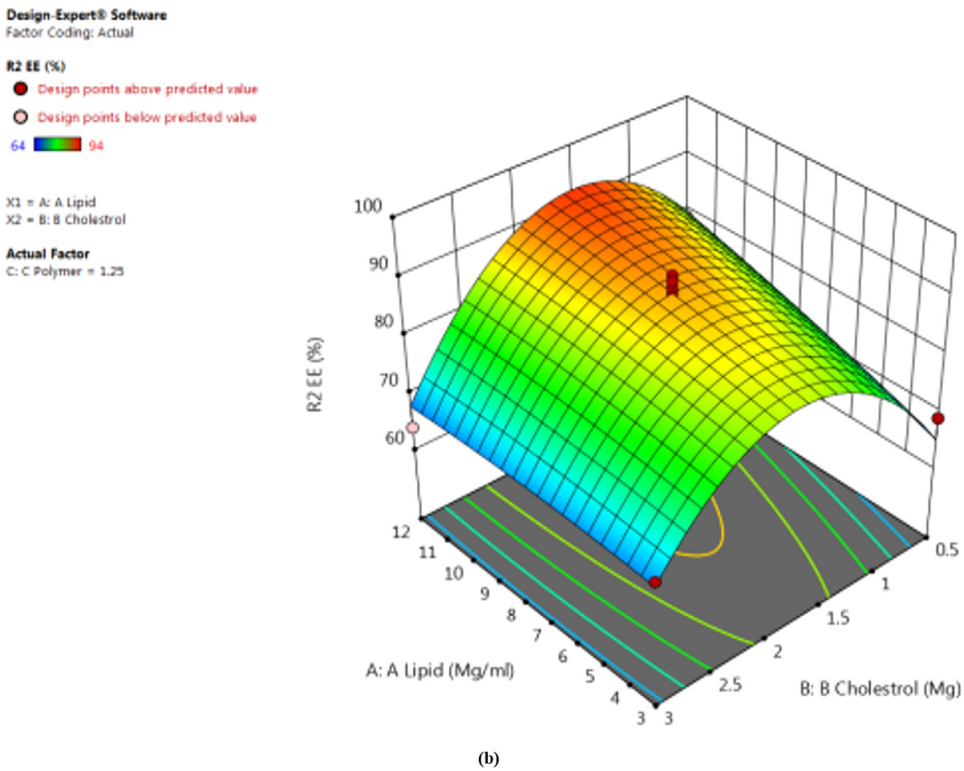

(b)

Figure 6. Response surface plots of particle size (a), entrapment efficiency (b), and effect of independent variables on percentage drug release of venlafaxine liposomes (c).

stretching at 2934 cm^{-1}, carbonyl group C=O stretching at 1613.36 cm^{-1}, skeletal vibrations of the aromatic ring at 1511.91 cm^{-1}, methylene groups at 1469.56 cm^{-1}, and C–O and C–N stretching at 1244.27 cm^{-1}, 1178.09 cm^{-1}, and 1034.80 cm^{-1}. These characteristics of stretching bands were retained in the FT-IR spectra of the drug, chitosan, and the physical mixture. The final physical mixture formulation revealed no significant chemical drug–recipient interactions. The FT-IR spectra of pure VLF, chitosan, and physical mixtures containing active pharmaceutical ingredients and excipients are depicted in Figure 4.

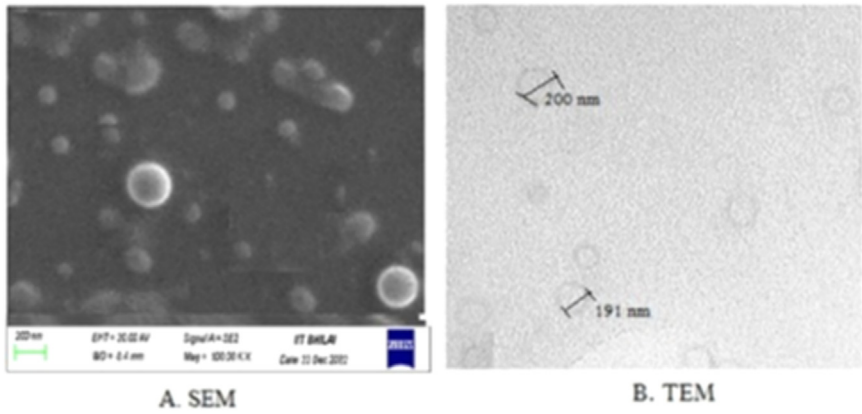

Figure 7. Optimized venlafaxine liposome images of scanning electron microscopy (SEM) (a) and transmission electron microscopy (TEM) (b).

Table 4
Summary result of regression analysis for variables like Df (degrees of freedom), SS (Sum of squares), Ms (Mean of squares), *F*, *P* value, R^2, and *SD*.

Variable	Df	SS	Ms	*F*	*P* value	R^2	SD
Particle size (nm)							
Model	9	32,005.21	3556.13	7.12	0.0085	0.9015	22.36
Residual	7	3498.55	499.79	–	–	–	–
Total	16	35,503.76	–	–	–	–	–
% Entrapment efficiency							
Model	9	1924.22	213.80	7.33	0.0078	0.9040	5.40
Residual	7	204.25	29.18	–	–	–	–
Total	16	2128.47	–	–	–	–	–
% Drug release							
Model	9	2355.93	261.77	8.90	0.0044	0.9196	5.42
Residual	7	205.95	29.42	–	–	–	–
Total	16	2561.88	–	–	–	–	–

PS and polydispersity

The formulation's PS influences how well a drug is delivered via the intranasal route. However, due to tight epithelial cell junctions that open and shut in response to the activation of signaling processes, the LP PS ranges significantly influence assimilation via the nasal route.[34] Although this choice may seem insignificant in comparison to the preformulation process, the device influences the geometry, size, and velocity of the particle plume. These factors have a significant influence on delivery effectiveness.[35] The particle size distribution of a liposomal dispersion in the range of below 20 to over 200 nm.[36] The improved formulation's PS decreased when the liquid lipid content was increased. The improved formulation's average PS was determined to be 191 (34.71) nm; the PS distribution and zeta potential distribution can be seen in Figure 5, and the polydispersity index (PDI) value was found to be 0.281.

Zeta potential

The colloidal system's physical storage stability can be determined by analysing the zeta potential (ZP), or electric potential, at the shear plane. The ZP value is also known to influence drug loading and the *in vivo* performance of drugs because it may be involved in drug distribution and clearance. The formulation's ZP, which was determined to be –22.32 mV, shows that it is stable.[37]

EE

The thin film hydration (TFH) method created VLF-loaded lipid carriers, improving hydrophilic drugs' EE. Formulation entrapment efficiencies were found to be 94.12% (1.20%). The incorporation of VLF resulted in high EE due to its lipophilic nature.

Design and optimization of VLF-loaded lipid carrier systems by BBD

Seventeen experiments were performed using the BBD for the prepared 3-center formulations. The 3 dependent variables are included in the values. Size (in nanometers), EE (%), and % drug release (Y1, Y2, Y3) specifically, the drug release rates range from 191.31 to 315.29 nm, 69.54% to 94.13%, and 43.46% to 84.13%. The quadratic model obtained for the formulation was a good fit. Table 4 shows the R^2, SD, and percent coefficient of variation for each of the 3 responses. The response surface plots of particle size, EE, and the effect of independent variables on the percentage drug release of VLF-LPs are shown in 3-dimensional graphs in Figure 6.

The average PS for all 17 experiments was 193.78 nm, so these values fall between the minimum and maximum values of the size range of 191.31 to 200 nm.

Final coded factors

Response 1 (Y1): Independent variables' effects on PS

Table 3 shows that the average particle size for all 17 experiments was 193.78 nm, between the lowest and highest values in the size range of 191. 31 to 200 nm.

$$\text{PS (nm)} = +207.80 - 4.13X_1 \times 50.62X_2 \times 4.25X_3 \times 9.75X_1X_2 \times 4.00X_1X_3 \times 8.00X_2X_3 \times 3.77X_1^2 \times 49.73X_2^2 \times 7.53X_3^2$$

Based on the above polynomials, it may be concluded that increasing the total lipid concentration also increased the PS of the LPs. Due to the surfactant's decreased emulsification efficiency and increased particle aggregation.[38] However, increasing the lipid concentration decreased the viscosity and surface tension of the for-

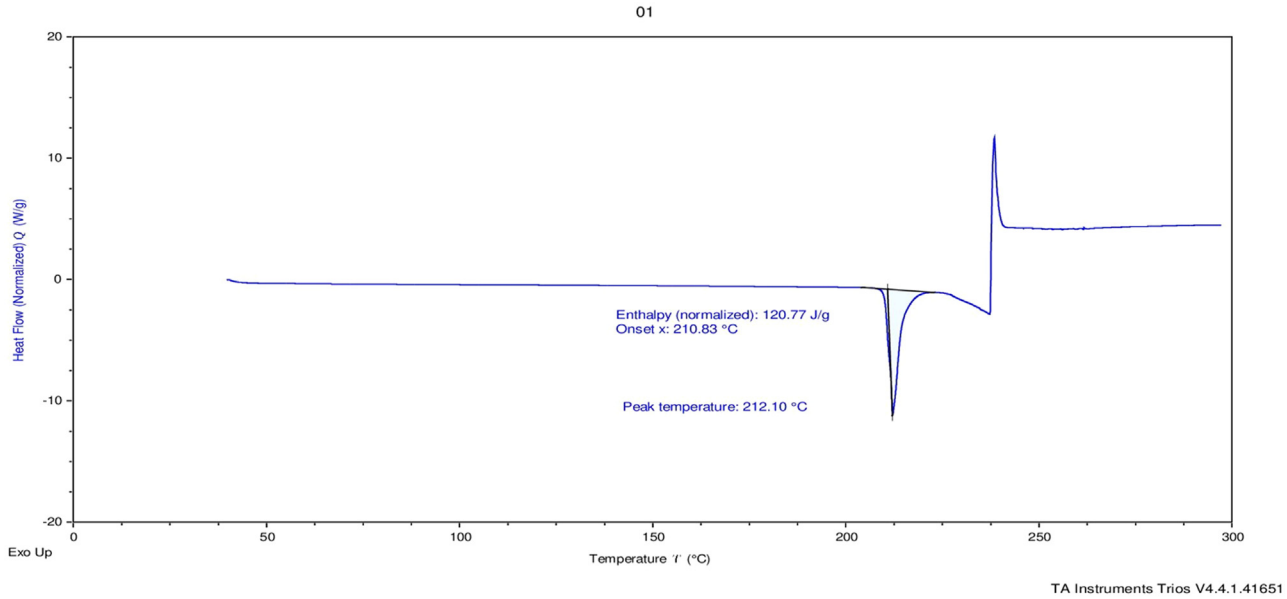

(a)

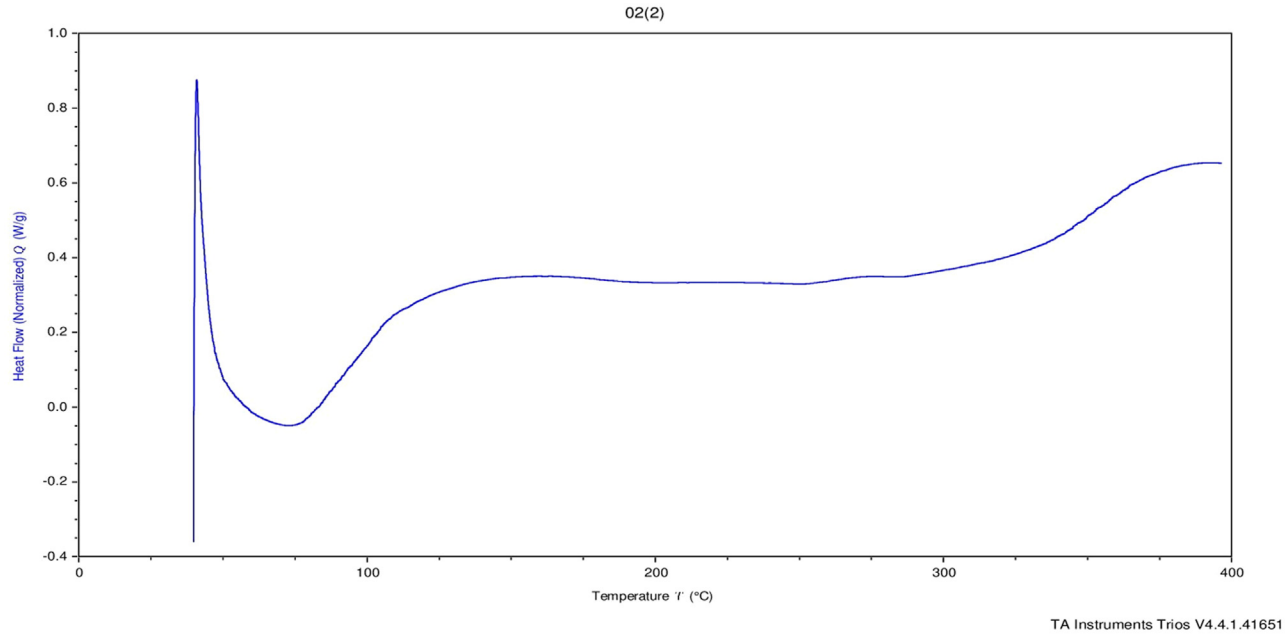

(b)

Figure 8. Differential scanning calorimetry thermal curves for pure drug (venlafaxine) (a), chitosan (b), and physical mixtures containing active pharmaceutical ingredients and excipients (c).

mulation, thus decreasing PS. Cholesterol had a slight effect on LP size.

$$EE\,(\%) = +89.00 + 3.62X_1 \times 2.25X_2 \times 2.63X_3 \times 3.75X_1X_2 \times 5.50X_1X_3 \times 6.25X_2X_3 \times 0.7500X_1^2 \times 18.00X_2^2 \times 0.7500X_3^2$$

Response 2 (Y2): independent variables' effects on %EE

Table 3 shows that the range of entrapment efficiency was 69. 54%–94. 12%.

According to the literature, increasing the total lipid concentration increases the EE, increasing the drug particle accommodation space. Furthermore, adding the lipid fraction reduces drug leakage into the external phase. The amount of lipids influences EE because an increase in lipids entraps the drug in the lipid core, thus increasing EE. The polymer concentration initially increases and can then decrease significantly as the surfactant molecules become trapped in the LPs.[39] Cholesterol has a slight effect on EE.

$$DR\,(\%) = +71.40 + 3.75 \times 1 \times 2.38 \times 2 \times 2.87 \times 3 \times 19.00 \times 1 \times 2 \times 0.5000 \times 1 \times 3 \times 3.75 \times 2 \times 3 \times 4.83X_1^2 \times 5.08X_2^2 \times 10.43X_3^2$$

Response 3 (Y3): The influence of independent variables on the percentage of drug release rate

As shown in Table 3, the percent drug release for all formulations developed ranged from 63% to 84.13%.

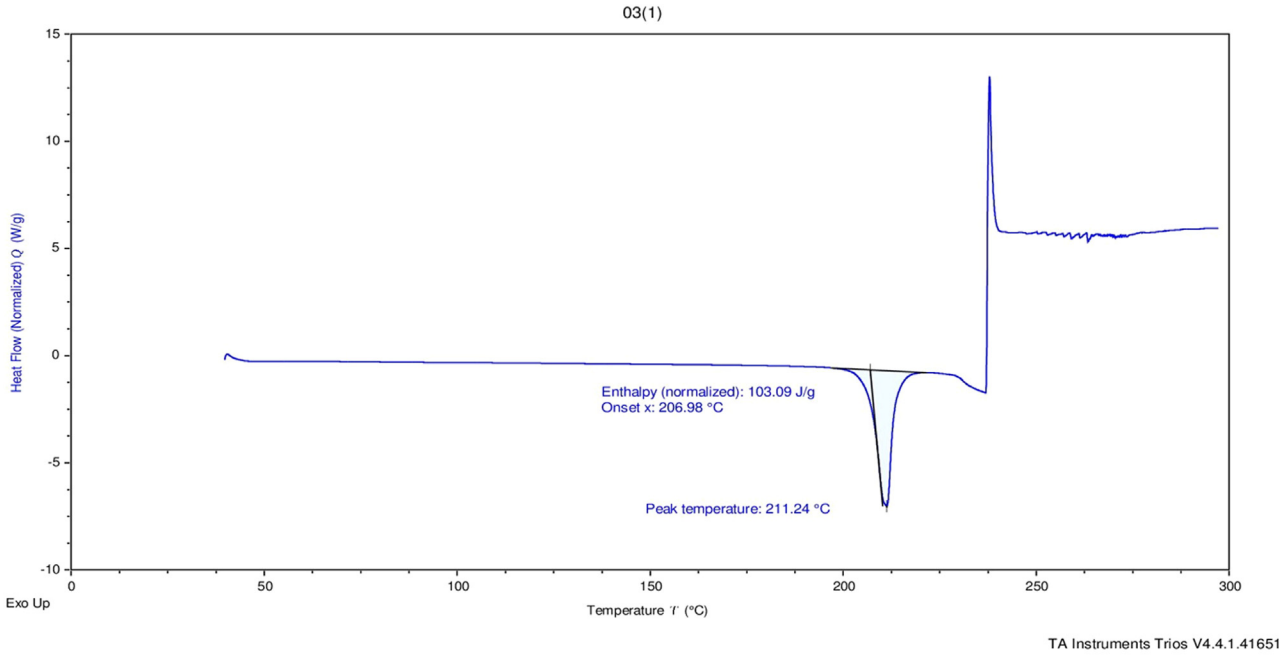

(c)

Figure 8. Continued

Table 5
Kinetic model that was used to predict the *in vitro* drug release pattern.

Parameter	Zero order	First order	Higuchi model	Korsemeyer-Peppas
R^2	0.5877	0.9813	0.9725	0.9747
R^2 adjusted	0.5877	0.9813	0.9724	0.9747
AIC	86.5974	90.1320	54.9589	10.015
MSC	2.0618	11.0524	0.6896	0.3162
Best fit values	k0: 5.402	k1: 0.010	kH: 16.393	kKP: 0.226

AIC = Akaike information criterion; MSC = Model Selection Criterion.

Total lipid and polymer concentrations greatly influenced the drug's *in vitro* release patterns from LPs. Drug release is accelerated by an increase in the concentration of lipids, whereas an increase in the concentration of polymers slows it down. The optimized LP formulation is based on the BBD design point prediction method. The optimized batch of the VLF-loaded LP had an average particle size of 201.4 nm, with %EE and percent drug release of 94.13% (1.2%) and 80.37% (1.4%), respectively. The particle size of 201.54 nm, trapping effectiveness of 94.53%, and drug release rate of 84.02% were determined to be valued reasonably close to those predicted by the BBD design.

SEM and TEM analysis

The morphology study revealed that the spherical shape and size of optimized VLF-LPs was 200 nm. These LPs resembled tiny pears in appearance. The formulation contains a mixed population of unilamellar vesicles and microvesicles containing optimized VLF-loaded LPs with a particle size of ~191 nm (~200 nm diameter) as measured by Zetasizer and showed a spherical shape. SEM and TEM images of optimized VLF-LPs are shown in Figure 7.

DSC analysis

DSC (Perkin Elmer Tyres, Waltham, Massachusetts) thermograms of the formulations were recorded. The DSC thermal curves for pure drug (ie, VLF), chitosan, and the physical mixtures containing active pharmaceutical ingredients and excipients are shown in Figure 8. The DSC thermogram of VLF showed a sharp endothermic peak at approximately 210 to 212°C, a smaller sharp peak at 214°C, and a broad peak at 246°C, indicative of polymorphism. A previous study identified different polymorphic forms of VLF with a heating rate of 2 K/min. The results indicate that the VLF used in this current study. Both cholesterol and chitosan had individual characteristics like an endothermic peak found for this cholesterol at 149°C and chitosan endothermic peak at 95°C and exothermic peak at 298°C. DSC was used to investigate the interaction between VLF and the polymer; no interaction was found.

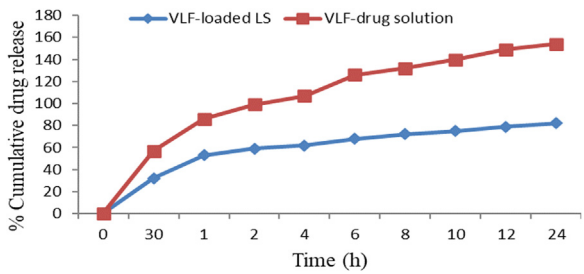

Figure 9. *In vitro* release profile of optimized venlafaxine (VLF)-loaded liposomes and VLF drug solution in simulated nasal fluid with pH 6.5. LPs (Liposome).

In vitro drug release

A dissolution test was performed using a membrane dialysis bag containing 250 mL phosphate buffered saline (pH 6.5), simu-

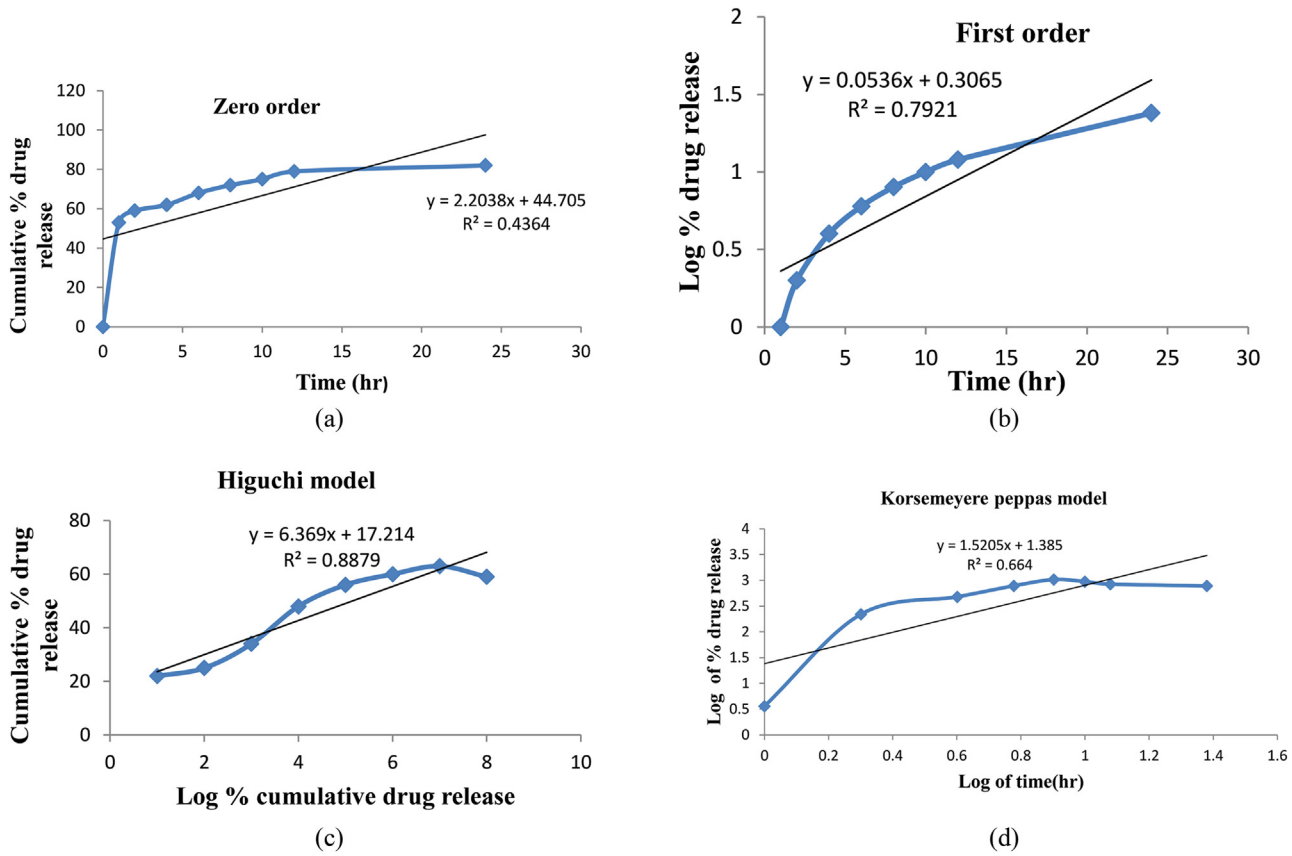

Figure 10. *In vitro* kinetic model of venlafaxine-loaded liposomes formulation: zero order (a), first order (b), Higuchi model (c), and Korsemeyer-Peppas model (d).

lating cerebrospinal fluid. The optimized VLF-LPs exhibited biphasic release from the prepared LPs and drug suspensions, with the fastest drug release rates during the initial stage from the lipid surface, followed by slower drug release due to degradation of the lipid core. The results showed a sustained release of the drug (54.1%) within the first hour; after that, the release was sustained from the optimized VLF-loaded LPs. The maximal drug release of VLF-loaded LPs was shown to be higher at 91.13% (1.023%) for up to 24 hours. It has been hypothesized that the initial burst of drug release may be due to nonentrapped VLF on the outer surface of the LPs. Hydrophilic drugs can rapidly diffuse through the hydrogel layer created by the chitosan-coated LPs exterior, rapidly absorbing water from the solution. After this initial phase, there was a delayed release phase in which the lipid core eroded, the chitosan shell dissolved, and the drug contained in the deep lipid matrix diffused into the release medium. Similar patterns were observed in the research on chitosan-coated methazolamide solid lipid nanoparticles (SLNs).[40]

Such a release pattern favours antidepressant targeting, and treatment of acute forms of depression requires a rapid onset (burst effect) followed by a slower release pattern to maintain therapeutic doses. Design of sustained release formulation that ensures the preferred VLF release from its LPs system, the drug release rate was analyzed using least-squares regression analysis. *In vitro* drug release profiles of optimized VLF-loaded LPs and VLF drug solutions in simulated nasal fluid (pH 6.5) are depicted in Figure 9. LPs are a well known and popular delivery system among researchers for targeting drugs to specific sites of action. Their powerful and unique ability to cross the blood-brain barrier and deliver drugs to target sites has been widely used for brain targeting. This effectively improved the loaded drug's absolute bioavailability, retention time, and intracerebral delivery. Various modifications are currently being made to the LPs' surface to improve its ability to target the brain. Neurologists and scientists have studied its use as a delivery system to treat brain disorders. This advanced approach to intranasal drug delivery has been shown to reduce the severity of encephalopathy and help restore normal neural function in the neural tube.[41] Although this venlafaxine-encapsulated LP drug delivery system offers a very interesting and successful approach to antidepressant therapy, further *in vitro* and *in vivo* studies are needed to make this a useful strategy for clinical trials.

In vitro release kinetic model of VLF-loaded LPs formulation

The *in vitro* kinetic models of VLF-loaded LPs formulation is zero order, first order, Higuchi model, and Korsmeyer-Peppas model shown in Figure 10. The R^2 values for the Higuchi and Korsmeyer-Peppas models for VLF-loaded LPs were 0.436, 0.792, 0.887, and 0.667, respectively. The R^2 values are near unity in the Higuchi model (0.887%); it was selected as the best-suited model (depicted in Table 5). This research work is designed to optimize and characterize antidepression drug VLF-loaded LPs, which will be further used for direct nasal-to-brain delivery.

Storage stability

Stability tests were performed according to the international council for harmonisation of technical requirements for pharmaceuticals for human use (ICH) Guideline Q1 A to achieve atmospheric storage conditions for the prepared formulation. This Guideline recommends stability testing parameters; that is, optimized particle size, drug release studies, and EE. These studies found an insignificant or minor increase in PS (from 191.31 to 194.61 nm during 3 months of storage at 4°C and 25°C). Similar results were observed at 25°C regarding drug release values (from

84.13 to 82.01%). The %EE of the optimized batch was 94.53% initially and 78.14% after storage at 4°C and 25°C for 3 months, respectively. There were no significant changes in LPs size, drug release, or encapsulation during LPs storage. Therefore, it was stable for a total of 3 months under the storage conditions tested (4 and 25°C).[42]

Conclusions

The recent study assessed the optimization of VLF-loaded LPs and further planned to manage depression. VLF-loaded LPs were successfully prepared by the TFH method followed by a rotary evaporator. Response surface methodology was used for experimental design, and BBD was used for optimization. The study aimed to develop a more affordable, biodegradable, and stable nanocarrier with increased drug EE and delayed release patterns. The drug release follows the kinetic model (R^2 value) of zero order, first order, and Higuchi and Korsmeyer-Peppas models for VLF-loaded LPs were determined to be 0.436, 0.792, 0.887, and 0.667, respectively. The R^2 values are near the unity of the Higuchi model (0.887%), and it was selected as the best-suited model. This research work was designed to optimize and characterize VLF-loaded LPs. The results suggest further *in vivo* studies of delivering VLF into the brain by administering it through the intranasal route. Our preliminary research conclusion is that intranasal drug administration of VLF-loaded LPs through nanocarriers could be an effective and more proficient approach for managing depression.

Declaration of Competing Interest

The authors have indicated that they have no conflicts of interest regarding the content of this article.

CRediT authorship contribution statement

Sulekha Khute: Data curation, Writing – original draft. **Rajendra K. Jangde:** Supervision, Methodology, Conceptualization, Validation, Writing – review & editing.

Acknowledgment

The authors are thankful to the HOD of the Institute of Pharmacy, Pt. Ravishankar Shukla University, Raipur, Chhattisgarh, India for providing the facility for this research work. Authors also acknowledge NIPER, Hajipur for providing the DSC facility, the SEM facility provided by the IIT Bhilai and the TEM facility provided by the AIIMS, New Delhi, India

References

1. He X, Yang L, Wang M, Zhuang X, Huang R, Zhu R, et al. Targeting the endocannabinoid/CB1 receptor system for treating major depression through antidepressant activities of curcumin and dexanabinol-loaded solid lipid nanoparticles. *Cell Physiol Biochem*. 2017;42(6):2281–2294.
2. Gul M, Shah FA, us Sahar N, Malik I, ud Din F, Khan SA, et al. Formulation optimization, *in vitro* and *in vivo* evaluation of agomelatine-loaded nanostructured lipid carriers for augmented antidepressant effects. *Colloids Surf. B.*. 2022;216:112537.
3. Dange SM, Kamble MS, Bhalerao KK, Chaudhari PD, Bhosale AV, Nanjwade BK, et al. Formulation and evaluation of VLF nanostructured lipid carriers. *J Bionanoscience*. 2014;8(2):81–89.
4. Dwivedi RK, Kushwaha SKS, Rai AK, Kushwaha N, Dwivedi D, Srivastava S. Development of novel formulation for intranasal delivery containing antidepressant agent. *Saudi J. Med. Pharm Sci.*. 2021;7(8):358–367.
5. Mukherjee S, Madamsetty VS, Bhattacharya D, Roy Chowdhury S, Paul MK, Mukherjee A. Recent advancements of nanomedicine in neurodegenerative disorders theranostics. *Adv. Funct. Matter.*. 2020;30(35):1–27.
6. Ali L, Ahmad M, Naeem M, Usman M, Akhtar M, Yousuf M, et al. Venlafaxine-loaded sustained-release poly (hydroxyethyl methacrylate- co -itaconic acid) hydrogel composites: their synthesis and *in vitro*/*in vivo* attributes. *Iran Polym J*. 2019.
7. Gutierrez MA, Stimmel GL, Aiso JY. Venlafaxine: a 2003 update. *Clin Ther*. 2003;25(8):2138–2154.
8. Zhi K, Raji B, Nookala AR, Khan MM, Nguyen XH, Sakshi S, et al. Plga nanoparticle-based formulations to cross the blood-brain barrier for drug delivery: From r&d to cgmp. *Pharm*. 2021;13(4):1–17.
9. Su Y, Sun B, Gao X, Dong X, Fu L, Zhang Y, et al. Intranasal delivery of targeted nanoparticles loaded with miR-132 to brain for the treatment of neurodegenerative diseases. *Front Pharmacol*. 2020;11:1–13.
10. Kashyap K, Shukla R. Drug delivery and targeting to the brain through nasal route: mechanisms, applications and challenges. *Curr Drug Deliv*. 2019;16(10):887–901.
11. Beule AG. Physiology and pathophysiology of respiratory mucosa of the nose and the paranasal sinuses. *GMS current topics in Otorhinolaryngology, head and neck surgery*. 2010:9.
12. Jangde RK, Khute S, Bhardwaj H, Yadav K. Development of nanoformulations for targeted transport of CNS drugs with greater pharmacological activity via the nose into the brain. *Int. J Drug Dev. Res.*. 2022;12(14):984.
13. Salib RJ, Howarth PH. Safety and tolerability profiles of intranasal antihistamines and intranasal corticosteroids in the treatment of allergic rhinitis. *Drug Safety*. 2003;26:863–893.
14. Bhise SB, Yadav AV, Avachat AM, Malayandi R. Bioavailability of intranasal drug delivery system. *Asian Journal of Pharmaceutics*. 2008;2(4).
15. Ul Islam S, Shehzad A, Bilal Ahmed M, Lee YS. Intranasal delivery of nanoformulations: A potential way of treatment for neurological disorders. *Molecules*. 2020;25(8):1–27.
16. Has C, Sunthar P. A comprehensive review of recent preparation techniques of liposomes. *J Liposome Res*. 2020;30(4):336–365.
17. Rahisuddin SP, Garg G, Salim M. Review of nasal drug delivery system with recent advancement. *Int J Pharm Pharm Sci*. 2011;3(2):1–5.
18. Mallick A, Sahu R, Nandi G, et al. Development of liposomal formulation for controlled delivery of valacyclovir: an *in vitro* study. *J Pharm Innov*. January 5, 2023 [Epub ahead of print].
19. Ahmed S, Amin MM, Sayed S. A comprehensive review on recent nanosystems for enhancing antifungal activity of fenticonazole nitrate from different routes of administration. *Drug Deliv*. 2023;30(1):2179129.
20. Al Badri YN, Chaw CS, Elkordy AA. Insights into asymmetric liposomes as a potential intervention for drug delivery including pulmonary nanotherapeutics. *Pharm*. 2023;15(1):294.
21. El Maghraby GM, Barry BW, Williams AC. Liposomes and skin: from drug delivery to model membranes. *Eur J Pharm Sci*. 2008;34(4-5):203–222.
22. Dugad A, Nalawade P, Thakhre R, Kakade S. Ion exchange resins: a novel approach towards taste masking of bitter drugs and sustained release formulations with their patents. *J Curr Pharma Res*. 2018;9(1):2656–2675.
23. Tamai I, Tsuji A. Transporter-mediated permeation of drugs across the blood–brain barrier. *J Pharm Sci*. 2000;89(11):1371–1388.
24. El-Far M, Elshal M, Refaat M, El-Sherbiny IM. Antitumor activity and antioxidant role of a novel water-soluble carboxymethyl chitosan-based copolymer. *Drug Dev Industrial Pharm*. 2011;37(12):1481–1490.
25. Soleymani SM, Salimi A. Enhancement of dermal delivery of finasteride using microemulsion systems. *Adv Pharmaceut Bull*. 2019;9(4):584.
26. Morrissey DV, Lockridge JA, Shaw L, Blanchard K, Jensen K, Breen W, Hartsough K, Machemer L, Radka S, Jadhav V, Vaish N. Potent and persistent *in vivo* anti-HBV activity of chemically modified siRNAs. *Nature Biotechnol*. 2005;23(8):1002–1007.
27. Marlowe JL, Akopian V, Karmali P, Kornbrust D, Lockridge J, Semple S. Recommendations of the oligonucleotide safety working group's formulated oligonucleotide subcommittee for the safety assessment of formulated oligonucleotide-based therapeutics. *Nucleic Acid Ther*. 2017;27(4):183–196.
28. Piel C, Quante A. Therapy strategies for late-life depression: a review. *J Psychiatr Pract*. 2023;29(1):15–30.
29. Xiang B, Cao DY. Preparation of drug liposomes by thin-film hydration and homogenization. *Liposome-based drug delivery systems*. 2021:25–35.
30. Agrawal M, Saraf S, Pradhan M, Patel RJ, Singhvi G, Alexander A. Design and optimization of curcumin loaded nano lipid carrier system using Box-Behnken design. *Biomed. Pharmacothe.*. 2021;141:111919.
31. Jazuli I, Nabi B, Alam T, Baboota S, Ali J. Optimization of nanostructured lipid carriers of lurasidone hydrochloride using Box-Behnken design for brain targeting: *in vitro* and *in vivo* studies. *J Pharm Sci*. 2019;108(9):3082–3090.
32. Jawahar N, Hingarh PK, Arun R, et al. Enhanced oral bioavailability of an antipsychotic drug through nanostructured lipid carriers. *Int J Biol Macromol*. 2018;110:269–275.
33. Saghafi Z, Mohammadi M, Mahboobian MM, Derakhshandeh K. Preparation, characterization, and *in vivo* evaluation of perphenazine-loaded nanostructured lipid carriers for oral bioavailability improvement. *Drug Dev IND Pharm*. 2021;47(3):509–520.
34. Jangde R, Elhassan GO, Khute S, Singh D, et al. Hesperidin-loaded lipid polymer hybrid nanoparticles for topical delivery of bioactive drugs. *Pharm*. 2022;15(2):211.
35. Deruyver L, Rigaut C, Lambert P, Haut B, Goole J. The importance of pre-formulation studies and of 3D-printed nasal casts in the success of a pharmaceutical product intended for nose-to-brain delivery. *Advanced drug delivery reviews*. 2021;175:113826.
36. Liu Y, Matida EA, Johnson MR. Experimental measurements and computational modeling of aerosol deposition in the Carleton-Civic standardized human nasal cavity. *Journal of Aerosol Science*. 2010;41(6):569–586.

37. Chin LY, Tan JY, Choudhury H, Pandey M, et al. Development and optimization of chitosan coated nanoemulgel of telmisartan for intranasal delivery: A comparative study. *J Drug Deliv Sci Technol*. 2021;62:102341.
38. Yasir M, Chauhan I, Zafar A, Verma M, et al. Buspirone loaded solid lipid nanoparticles for amplification of nose to brain efficacy: Formulation development, optimization by Box-Behnken design, in-vitro characterization and in-vivo biological evaluation. *J. Drug Deliv. SCI. Technol.*. 2021;61:102164.
39. Apostolou M, Assi S, Fatokun AA, Khan I. The effects of solid and liquid lipids on the physicochemical properties of nanostructured lipid carriers. *Journal pharmaceutical sciences*. 2021;110(8):2859–2872.
40. Alshweiat A, Csóka I, Tömösi F, Janáky T, Kovács A, et al. Nasal delivery of nanosuspension-based mucoadhesive formulation with improved bioavailability of loratadine: preparation, characterization, and *in vivo* evaluation. *Int. J. Pharm.*. 2020;579:119166.
41. Agrawal M, Tripathi DK, Saraf S, Saraf S, Antimisiaris SG, Mourtas S, Margareta HU, Alexander A, et al. Recent advancements in liposomes targeting strategies to cross the blood-brain barrier (BBB) for the treatment of Alzheimer's disease. *J Control Release*. 2017;260:61–77.
42. El-Samaligy MS, Afifi NN, Mahmoud EA. Evaluation of hybrid liposomes-encapsulated silymarin regarding physical stability and *in vivo* performance. *Int J Pharmaceutics*. 2006;319(1-2):121–129.